

# On the Application of Probabilistic Decline Curve Analysis to Unconventional Reservoirs

U. C. Egbe<sup>1</sup>, O. O. Awoleke<sup>1</sup>, O. M. Olorode<sup>2\*</sup>, and S. D. Goddard<sup>1</sup>

<sup>1</sup>University of Alaska Fairbanks

<sup>2</sup>Louisiana State University

## Summary

Several authors have worked on combining decline curve analysis (DCA) models and stochastic algorithms for probabilistic DCAs. However, there are no publications on the application of these probabilistic decline curve models to all the major shale basins in the United States. Also, several empirical and analytical decline curve models have been developed to fit historical production data better; there is no systematic investigation of the relevance of the efforts on new model development compared with the efforts to quantify the uncertainty associated with the “noise” in the historical data. This work compares the uncertainty associated with determining the best-fit model (epistemic uncertainty) with the uncertainty associated with the historical data (aleatoric uncertainty) and presents a procedure to find DCA-stochastic algorithm combinations that encompass the epistemic uncertainty.

We investigated two Bayesian methods—the approximate Bayesian computation and the Gibbs sampler—and two frequentist methods—the conventional bootstrap (BS) and modified BS (MBS). These stochastic algorithms were combined with five empirical DCA models (Arps, Duong, power law, logistic growth, and stretched exponential decline) and the analytical Jacobi theta-2 model. We analyzed historical production data from 1,800 wells (300 wells from each of the six major shale basins studied) with historical data lengths ranging from 12 to 60 months. We show the errors associated with the assumption of a uniform distribution for the model parameters and present an approach for integrating informative prior (IP) probabilistic distributions instead of the noninformative prior (NIP) or uniform prior distributions. Our results indicate the superior performance of the Bayesian methods, especially at short hindcasts (12–24 months of production history). We observed that the duration of the historical production data was the most critical factor. Using long hindcasts (up to 60 months) leveled the performance of all probabilistic methods regardless of the decline curve model or statistical methodology used. Additionally, we showed that it is possible to find DCA-stochastic model combinations that reflect the epistemic uncertainty in most of the shale basins investigated.

The novelty of this work lies in the development of IPs for the Bayesian methodologies and the development of a systematic approach to determine the combination of statistical methods and DCA models that encompasses the epistemic uncertainty. The proposed approach was implemented using open-source software packages to make our results reproducible and to facilitate its practical application in forecasting production in unconventional oil and gas reservoirs.

## Introduction

Several models have been developed to forecast oil and gas production from unconventional oil and gas reservoirs. These include numerical, analytical, and semianalytical methods that solve a system of partial differential equations, as well as several empirical methods that are fitted to historical production data. Numerical simulation methods are considered the most accurate and reliable forecasting methods (Makinde and Lee 2016) because of their ability to model the complex physics of flow in petroleum reservoirs. However, their application is typically time-consuming and computationally expensive, which curtail its application where time and computational resources are limited. Considering that unconventional oil and gas reservoirs are commercially developed with hundreds of multistage fractured horizontal wells, most petroleum engineers resort to using analytical, empirical, semianalytical, and data-driven models to predict petroleum production performance efficiently.

Most analytical methods seek closed-form solutions to the partial differential equations that govern flow in porous media. A recent example of this approach is described in Holanda et al. (2018), where the authors present a physics-based model that accounts for the material balance and linear flow in hydraulically fractured horizontal wells. They used the second Jacobi theta function to simplify the infinite summation in the resulting analytical solution to the governing partial differential equation. The resulting model has three parameters and was shown to forecast production reliably. Hazlett et al. (2021) also developed an analytical model that captures the different flow regimes in a petroleum reservoir. This model was derived from Hazlett and Babu’s transient well pressure solution (Hazlett and Babu 2014, 2018) for uniform pressure wells and the Farooq et al. (2020) single-fracture model. The model has four parameters that are not independent and together model the transition of flow in a reservoir. The model showed a good fit to production data but is yet to be tested on many wells. Hazlett et al. (2021) also opined that their model would be difficult to invert using a method like regression analysis because of the presence of multiple/nested exponentials in their solution.

Makinde and Lee (2016) presented a semianalytical technique that also utilized principal component methodology. Singular value decomposition is used to calculate the production data’s principal components, and the results were used to forecast production. Although this model performed well with minimal production history (6 months), the prediction error increased with increasing production history.

The DCA approach started as an empirical method for forecasting production or petroleum reserves. The Arps model is the most used DCA method because of its relative simplicity (Arps 1945). The Arps equation assumes boundary-dominated flow (BDF), which is the most prevalent flow regime in conventional reservoirs. However, unconventional reservoirs (such as shales and tight sands) are typically used in transient linear flow during most of their production life. Depending on the distance between the fracture stages, this transient flow

\*Corresponding author; email: [olorode@lsu.edu](mailto:olorode@lsu.edu)

Copyright © 2022 Society of Petroleum Engineers

Original SPE manuscript received for review 20 August 2022. Revised manuscript received for review 13 October 2022. Paper (SPE 212837) peer approved 17 October 2022. Supplementary materials are available in support of this paper and have been published online under Supplementary Data at <https://doi.org/10.2118/212837-PA>. SPE is not responsible for the content or functionality of supplementary materials supplied by the authors.

typically transitions into the fracture-interference flow regime, where the pressure drops around each fracture stage begin to interfere with those from the neighboring fracture stages but rarely transition to the expected late-time BDF at the end of the well life. The expected long duration of the linear flow regime in these hydraulically fractured tight rocks makes the Arps model predictions overly optimistic because it was developed with the assumption of BDF (Lee and Sidle 2010). Therefore, several researchers have developed newer models to overcome the shortcomings of the Arps model.

These second-generation DCA models include the Duong model (Duong 2011), logistic growth analysis (LGA) model by Clark et al. (2011), stretched exponential production decline (SEPD) model by Valkó and Lee (2010), and power law exponential (PLE) model by Ilk et al. (2008). Hybrid models, which combine different DCA models, have also been developed to model production profiles from shale oil and gas reservoirs accurately. In these hybrid models, heuristic approaches help identify the dominant flow regimes and determine when to apply each model. For example, Okouma et al. (2012) used diagnostic plots from four different rate-time equations to obtain the DCA model parameters. They studied three shale plays and got different results with the log-log plot of rate vs. time. A clear linear flow trend with a negative half slope was observed in one of the shales. However, a BDF with a negative unit slope was observed in another shale play after 100 days of production. Khanal et al. (2015) showed that using a log-log diagnostic plot of rate vs. time to identify linear flow could lead to misleading results. They recommended using a log-log plot of pressure-normalized rate vs. time to identify linear and bilinear flow regimes and a log-log plot of pressure-normalized rate vs. material balance time to identify the BDF regime more accurately. They noted that there is no consensus on what model to use for the transition period, so they used models designed for linear flow.

Additionally, they proved that a combination of SEPD and Arps gave a more accurate production forecast than single models alone. Makinde and Lee (2016) used diagnostic plots to determine when to apply hybrid models. They used log-log plots of rate vs. time and rate vs. material balance time. Both plots (especially the latter) showed lengthy periods of transition flow, but contrary to Khanal et al. (2015), they modeled the transition flow with the Arps model. They concluded that hybrid DCA models performed better than standalone DCA models for forecasting production. Despite the advantages of the hybrid models, their limitation is that we typically do not know when to apply the different models that make up the hybrid model. Diagnostic plots offer some help but are left to subjective interpretation and induce a human bias in interpreting these plots. There is also the challenge of accurately modeling the transition flow periods that can occur for a long time because there are no known models to fit this flow regime adequately. These issues result in an increased vulnerability to errors and uncertainties in the forecasts and underscore the need for uncertainty quantification in production forecasting.

Uncertainty can be defined as the range of possible values within which we can be reasonably certain that the true value of an estimated quantity lies. It can be characterized as epistemic or aleatoric (Der Kiureghian and Ditlevsen 2009). Aleatoric or statistical uncertainty results from randomness inherent in an observable process (Choi et al. 2020). Therefore, even with complete knowledge of the most appropriate model for the data-generating mechanism, there is still some uncertainty in the actual outcome of an event. Epistemic (or systemic) uncertainty arises from the lack of knowledge of the underlying model. So, the assumptions made during the development of a model are sources of epistemic uncertainties because they indicate a lack of knowledge about the phenomenon being modeled. Der Kiureghian and Ditlevsen (2009) noted the difficulty of classifying uncertainties as either aleatoric or epistemic and mentioned that such a classification is subjective and dependent on the context and application. In this work, we will compare the epistemic uncertainty (in production forecasting owing to the choice of the deterministic DCA models) with the aleatoric uncertainty (in production forecasting resulting from implementing probabilistic techniques with various DCA models). To this end, we introduce and discuss the probabilistic uncertainty quantification methods used in this study.

The frequentist and Bayesian methodologies are the main approaches for probabilistic uncertainty quantification in the petroleum engineering literature. Several authors have found that applying these methodologies can effectively quantify uncertainty in production forecast and reserves estimation. Jochen and Spivey (1996) applied the BS method with varying sample sizes to quantify production forecast uncertainty. They assumed that the production data were independent and identically distributed. Cheng et al. (2010) found this assumption improper for time-series data because the data structure contains correlations among data points. They proved that the BS method was unreliable for quantifying uncertainty in production forecast, and that the actual reservoir estimates lie outside the P90-P10 80% confidence interval more than 20% of the time. So, they developed a modified version called the modified bootstrap (or MBS as denoted in this paper) method and applied it to the Arps model to address this limitation of the BS methodology. Their results proved that the MBS yielded a more accurate quantification of production forecast uncertainty with much wider confidence intervals and improved realized coverage rate (CR) of the confidence intervals. However, the CRs did not improve as more production data were available for history matching even though the confidence interval became narrower.

Okoli (2020) applied the BS and the MBS methodologies to three different DCA models—Arps, SEPD, and Duong—in three shale basins. They used different BS sample sizes, ranging from 10 to 10,000, and the CR and P50 error prediction did not improve significantly with varying BS sample sizes. However, their results for the application of different combinations of models in each shale basin indicated that the BS method outperformed the MBS method. They did not present the Duong model and the BS method results because they were unrealistic. A drawback of the frequentist probabilistic approach is that it does not take in any prior knowledge of the DCA model parameters—an issue that the Bayesian probabilistic approach solves.

Gong et al. (2014) applied the Bayesian probabilistic methodology to the Arps model using the Markov chain Monte Carlo (MCMC) sampling with the Metropolis-Hastings algorithm on 167 wells in the Barnett Shale. They assumed that the parameters of the Arps model were independent uniform distributions with constraints. The Markov chain's initial parameters were obtained from parameter estimation after curve fitting the Arps model to the historical production data. They defined their proposed distribution for the Arps parameters using a set of standard deviations, which they believed provided good mixing for the MCMC sampler. They ran the Markov chain for 1,000 iterations and used the values from the posterior distribution of the parameters to make a probabilistic production forecast. They showed that their approach was faster than the MBS method (Cheng et al. 2010) and performed better in nearly every aspect.

Gonzalez et al. (2012) expanded the approach presented in Gong et al. (2014) to different DCA models on 197 horizontal gas wells in the Barnett Shale. They performed the analysis using six hindcast sizes ranging from 6 to 36 months with a 6-month step. They defined each DCA model's prior distribution using independent and uniform distributions. Their definitions of the likelihood and posterior distributions were the same as in Gong et al. (2014). They concluded that uncertainty and prediction errors were reduced with increasing hindcast size. However, the predictions were biased and unrealistic for specific models when using fewer than 12 months of hindcast size. Their work also showed that P50 estimates using the Bayesian approach were more accurate than deterministic estimates at early times. Gonzalez et al. (2012) conducted two experiments where they compared the performance of the Metropolis-Hastings algorithm using informative and noninformative DCA LGA model parameters. One of the experiments used an informative carrying capacity, while the other used a uniform noninformative carrying capacity. They left the remaining LGA parameters' prior distribution uniform in both cases. The IP distribution for the  $K$  parameter was obtained from other sources (Clark et al. 2011). Their result showed that the accuracy and calibration of probabilistic production forecasts were further enhanced when using IPs.

Paryani et al. (2017) applied the approximate Bayesian computation (ABC) methodology to quantify the uncertainty associated with the Arps and LGA DCA models in production forecasting. Their methodology is more straightforward than the MCMC sampling with the Metropolis-Hastings algorithm because it does not require evaluating the likelihood function. They created a simulated data set with constrained uniform distribution for the prior distribution of the DCA model parameters. They used a distance measure (mean, standard deviation) between the simulated and the observed data for the likelihood function and the rejection sampling technique to set the threshold to accept or discard the simulated production data. Paryani et al. (2017) concluded that the ABC methodology was computationally faster than the likelihood-based Bayesian methodology and provided more accurate results with the DCA models than the deterministic methods. Korde et al. (2021) expanded Paryani et al. (2017) and Gong et al. (2014) to other DCA models and implemented the Gibbs sampling algorithm as a different Bayesian probabilistic methodology. Their work was based on more than 74 oil and gas wells in the Permian Basin. The prior distribution for the three Bayesian methods they studied was uninformative uniform distributions. They proved that the probabilistic models performed better in all aspects as more production history data became available. The CR for the Permian Basin was between 80 and 100%, but because of their use of NIPs, the interval between the P90 and P10 bounds was unsatisfactorily wide.

In this work, we develop an automated Bayesian workflow to address the shortcomings of applying the Bayesian methodology to production forecasting and uncertainty quantification. This work provides an objective and straightforward statistical approach of using several DCA models (one analytical and five empirical) to estimate reserves or production forecasts from given production rate-time data. To eliminate human bias, we automated the workflow in R (R Core Team 2020) and used “unbiased” IPs from a data set of more than 300 shale wells per basin to improve the accuracy and uncertainty quantification of the Bayesian algorithms applied. We extend the application of the frequentist (BS and MBS) and Bayesian probability statistics (ABC and Gibbs sampling) to common DCA models for shale plays to evaluate their performance and trends. Additionally, we investigated the effect of the IP distribution of DCA model parameters on model performance. Finally, we compared aleatoric and epistemic uncertainties to recommend the DCA-stochastic algorithm pairs that encompass the epistemic uncertainty in the shale basins investigated.

## Data Collection and Cleaning

This work leverages production data from several US shale oil and gas operating companies, which are reported in the software-as-a-service provided by Enverus. The data include monthly oil production rates from multistage fractured horizontal wells in Texas, New York, Pennsylvania, North Dakota, Montana, Louisiana, and Wyoming. Although daily rates were unavailable, the monthly production data used have the advantage of being less noisy and making our production hindcast and forecast algorithms much faster than if daily rates are used. The Enverus data repository does not contain a temporal record of bottomhole pressure data. As such, it will be interesting to check (in future work) how the results of this analysis could change when pressure-normalized rate vs. time data is used instead of rate vs. time data. To test the robustness of the proposed probabilistic methodology, we used production data from various unconventional shale plays such as the Eagle Ford, Haynesville, Barnett, Marcellus, Bakken, and Permian basins. The steps to clean the data are outlined as follows:

1. We removed rows with one or more missing value(s).
2. We selected production data only from the desired shale basins.
3. We selected 300 wells from each of these shale basins based on the following criteria:
  - At least 96 months of production data. This is to ensure that we have an adequate number of wells with a statistically significant number of data points in each well’s production history.
  - We selected production wells with cumulative production values greater than 200 thousand bbl for oil wells and 1 MMscf for gas wells.

Considering that DCA was developed for wells with a natural production decline, we removed wells with sharp anomalous increases in production rates that are typically caused by shut-ins or refracturing. To achieve this, we only selected wells that meet all the following criteria:

1. The maximum production rate ( $q_{max}$ ) must be within the first 10 months of production. This is indicated as the first annotation in **Fig. 1**, where  $q_{t1}, \dots, q_{t10}$  represent the rates for the first 10 months, respectively.
2. The current production rate ( $q_{tn}$ ) must be less than twice the magnitude of the previous month’s production rate.
3. The absolute difference between two consecutive monthly production data points ( $q_{tn+1}$  and  $q_{tn}$ ) must be less than three folds of the standard deviation ( $sd$ ) of the production rate data for that well. This rule is a modified application of the three-sigma rule.

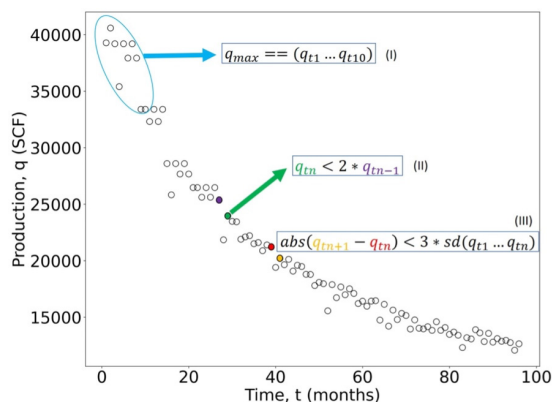


**Fig. 1—Graphical illustration of the criteria used to select wells with appropriate production decline.**

**Fig. 1** presents a rate-time plot that graphically illustrates these three criteria. Although several wells meet these criteria in each shale basin, we selected 300 wells (from each basin) to facilitate a reasonable comparison of the probabilistic analyses in this work.

## DCA Models and Parameter Ranges

We applied different popular DCA models to evaluate how well our approach performs on each one. To avoid the vulnerability to human bias typically associated with visual curve fitting, we automated the procedure of estimating the DCA model parameters using the Levenberg-Marquardt nonlinear least-squares algorithm in R (<https://www.rdocumentation.org/packages/minpack.lm/versions/1.2-2>). **Table 1** outlines the DCA models used in this work and provides references for further details.

Name	Type	Information
Arps	Empirical	Arps (1945)
Duong	Empirical	Duong (2011)
LGA	Empirical	Clark et al. (2011)
SEPD	Empirical	Valkó and Lee (2010)
PLE	Empirical	Ilk et al. (2008)
Jacobi 2 theta	Analytical	Holanda et al. (2018)

Table 1—Summary of DCA models used in this work.

**Table 2** presents a summary of the parameter bounds used in the regression algorithm to fit the DCA models to the historical production rates. These bounds, as discussed in Gong et al. (2014), Korde et al. (2021), and Holanda et al. (2018), give sufficient room for the probabilistic methods to explore the probable solution space. As shown in **Table 2**, all the DCA models use three parameters except the PLE, which uses four parameters. The  $q_i$ ,  $b$ ,  $D_i$  parameters in the Arps and Duong models represent the initial flow rate, decline exponent, and initial decline rate, respectively, whereas  $q_i$ ,  $a$ , and  $m$  represent the initial rate coefficient, model coefficient, and time exponent in the Duong model. The parameters  $K$ ,  $n$ , and  $a$  represent the carrying capacity, time exponent, and model coefficient in the LGA model, while  $q_i$ ,  $\eta$ , and  $\tau$  represent the initial rate coefficient, time exponent, and time coefficient in the SEPD model. In the Jacobi theta 2 model,  $q_i$ ,  $\eta$ , and  $X$  represent the virtual initial rate, reciprocal characteristic time, and geometric factor, respectively. Finally,  $q_i$ ,  $D_i$ ,  $D_\infty$ , and  $n$  represent the initial rate coefficient, decline coefficient, terminal decline coefficient, and time exponent in the PLE model.

DCA Model	Parameter	Lower Limit	Upper Limit
Arps	$q_i$	1	1,000,000
	$b$	0	2
	$D_i$	0.1	50
Duong	$q_i$	0.01	1,000,000
	$a$	0.5	5
	$m$	0.5	5
LGA	$K$	1,000	20,000,000
	$n$	0.01	5
	$a$	1	1,000
SEPD	$q_i$	1	1,000,000
	$\eta$	0.01	5
	$\tau$	1	100
Jacobi theta 2	$q_i$	1	1,000,000
	$\eta$	0.001	5
	$X$	0.001	10
PLE	$q_i$	1	1,000,000
	$D_i$	0.001	10
	$D_\infty$	$1 \times 10^{-9}$	1
	$n$	0.001	5

Table 2—DCA model parameter bounds.

## Bayesian Methodology

We applied the Bayesian approach to probabilistic production DCA using the Gibbs sampler (Korde et al. 2021) and the ABC algorithm (Paryani et al. 2017; Korde et al. 2021). The critical difference between these two algorithms is that the Gibbs sampler evaluates the likelihood, whereas the ABC algorithm simulates new data from the likelihood using the procedure described in Korde et al. (2021). The Bayesian methodology is based on the prior, likelihood, and posterior probability distributions. The following two subsections discuss the ABC and Gibbs algorithms, respectively.

**Approximate Bayesian Computation (ABC).** In Paryani et al. (2017) and Korde et al. (2021), the DCA model parameters were assumed to have a uniform prior distribution. This assumption is not necessarily representative of an analyst's beliefs, so we generated an IP

distribution for each Arps decline model parameter using a subset of the production data set. The results summarized in **Fig. 2** show that the distribution of the Arps model parameters is significantly different from a uniform distribution. The approach we used to estimate the prior distributions of the DCA model parameters helps avoid introducing errors into the production forecasting workflow. Additionally, we found that the proposed approach is not limited to the Arps DCA model but applies to all the other DCA model parameters. Our proposed method to generate representative and IP DCA model parameter distributions is summarized as follows:

1. Estimate the model parameters by fitting each DCA model to production data from one-third of the wells (100 wells out of the 300-well data set) in each basin using regression.
2. Use a kernel density estimator function in R to smooth the histogram of each DCA parameter and create a linear interpolation function. This is shown as the blue lines in **Figs. 2a through 2c**. We cannot use this density function directly in the workflow because it is not parameterized. To be able to parameterize it, we proceed to Step 3.
3. Generate parameter draws that are uniformly distributed within each parameter bound. The parameter bounds are set as in **Table 2**. The uniform distribution is shown as the horizontal black line in **Figs. 2d through 2f**.
4. Sample from the uniform parameter draws using the smoothed histogram developed in Step 2 as the probability of occurrence to estimate the desired prior probability distributions. This is a score transform—transforming the samples from the uniform distribution to the target distribution; the target distribution is the kernel density in Step 2.
5. The estimated distributions yield a better representation of the accurate model parameter distributions, as represented by the red line plots in **Figs. 2d through 2f**. These probability distributions are parameterized and are fed into the Bayesian algorithm as the prior distributions for the corresponding model parameters.

### Arps parameter distribution generated from a subset of production wells

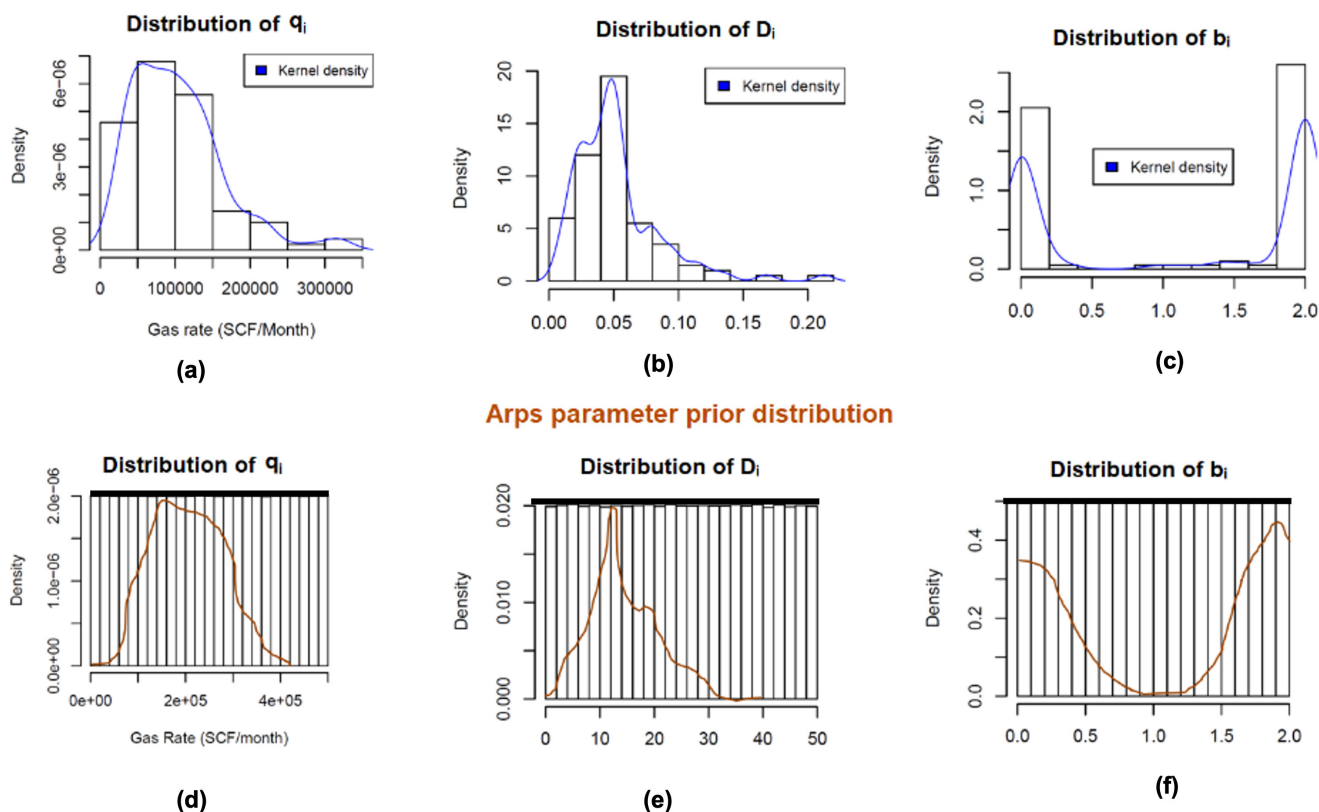


**Fig. 2—Illustration of the process for estimating IPs for Bayesian analysis.**

It is worth mentioning that the 100-well subset used to develop the IPs in each shale basin was neither used for production forecasting nor for evaluating the ABC algorithm’s performance. We did this to avoid misleading or biased conclusions on the algorithm’s performance because these 100 wells were used to estimate the prior probability distribution. **Fig. 3** illustrates how we apply the ABC algorithm in probabilistic DCA as in Paryani et al. (2017) and Korde et al. (2021). The summary statistics used to compare the simulated data to the actual data include the mean, median, absolute deviation, and standard deviation. Simulated data sets that are not within the set threshold limits were rejected. The maximum threshold value used is 0.01, meaning that only a 1% difference in the summary statistics is acceptable. In this work, we leveraged the “abc” package (Csilléry et al. 2010) in the R statistical programming language to facilitate the implementation of the ABC algorithm for DCA.

**Gibbs Sampler.** We refer the reader to Korde et al. (2021) for details regarding the Gibbs sampler and its implementation in petroleum production forecasting. Here, we present a new procedure to generate IP probability distributions for the Gibbs sampler as follows:

- Estimate model parameters by fitting each DCA model to one-third of the well production data in each basin using nonlinear regression.
- Collect summary statistics (mean, precision, and skewness) by following a procedure similar to the one outlined for computing IPs in the ABC section (**Fig. 2**).

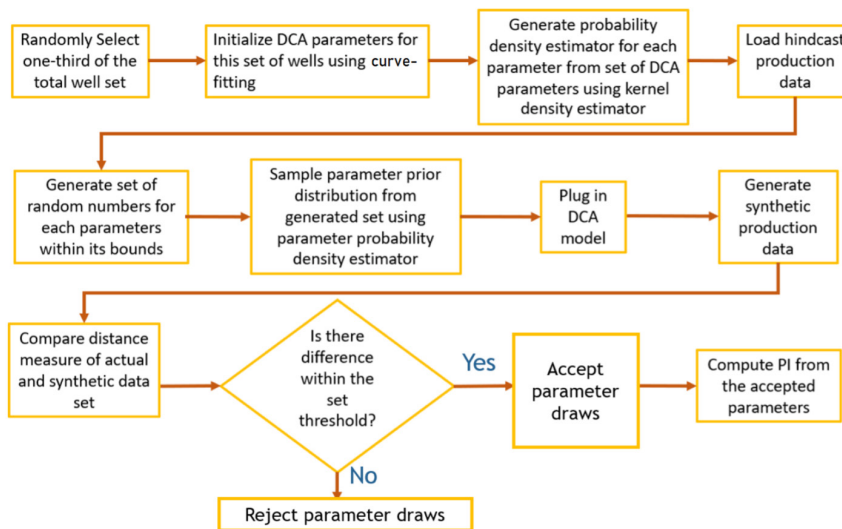


Fig. 3—Flow chart for ABC technique. PI = prediction interval.

We implemented the MCMC Gibbs sampler method using the OpenBUGS open-source software. We used 10,000 iterations and discarded the first 2,000 as a burn-in set. Fig. 4 summarizes the entire process of running the Gibbs sampler.

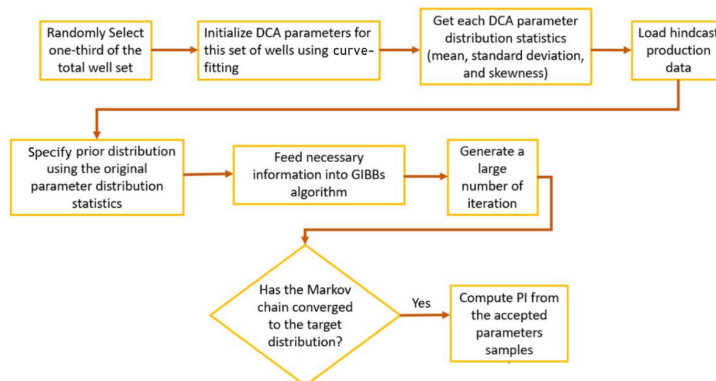


Fig. 4—Flow chart for the Bayesian MCMC method using the Gibbs sampler. PI = prediction interval.

### Frequentist Methodology—Conventional BS and MBS

The overall workflow for the conventional BS methodology using an arbitrary model is illustrated below (as discussed more exhaustively in Okoli 2020):

1. Set aside an initial fraction of the data set as the hindcast and reserve the remainder of the data set to estimate the misfit between predicted (forecast) and actual production.
2. From the initial hindcast production data set, generate multiple BS samples by randomly sampling with replacement. Each BS sample has the same size as the hindcast.
3. Estimate the parameters in the decline curve model by fitting the selected DCA model to the bootstrapped data using regression analysis.
4. Using the estimated parameters and the DCA model, forecast production performance.
5. Repeat Steps 1–4, iterating through all the BS samples.
6. Summarize the overall distribution of productivity/cumulation production by computing the distributions' 10th, 50th, and 90th percentiles.

In the conventional BS method, the production data are considered independent and identically distributed even though it is a sequence of time-dependent observations with a trend (thus not independent and identically distributed). To address this limitation, Cheng et al. (2010) introduced the “MBS method with block resampling.” The overall workflow for the MBS methodology with an arbitrary model is described as follows (Okoli 2020):

1. Set aside a fraction of the data set as the hindcast and reserve the remainder of the data set to estimate the misfit between predicted (forecast) and actual production.
2. Fit the initial hindcast data set with a decline curve model and compute the residuals between the fitted model and observed data.
3. Determine the optimal block size by applying an autocorrelation function (Cheng et al. 2010; Okoli 2020) to the residuals. Next, group the residuals into time intervals based on the optimal block size.
4. Generate multiple block BS samples of the residuals by randomly sampling the blocks with replacement. Each complete BS sample has the same size as the original hindcast.

5. Add the block BS samples of the residuals to the production fitted values to obtain BS production data.
6. Compute the parameters in the decline curve model by fitting the selected DCA model to the BS sample data using regression analysis.
7. Using the fitted model, forecast production performance.
8. Repeat Steps 4–7 until all the BS samples.
9. Summarize the overall distribution of productivity/cumulation production by computing the distributions' 10th, 50th, and 90th percentiles.

We refer our readers to the summary of Jochen and Spivey (1996), Cheng et al. (2010), and Okoli (2020) in the Introduction section of this paper for further details regarding the conventional BS and MBS methods. In this work, we implemented the conventional BS and MBS methods as presented in Okoli (2020).

## Uncertainty

Uncertainty can be defined as a lack of knowledge about the outcome of a random event or about the actual state of a phenomenon (Hubbard 2014). In petroleum production forecasting, sources of uncertainty can include (but are not limited to) the following (Begg et al. 2014 and Der Kiureghian and Ditlevsen 2009):

- Measurement of empirical quantities (production rate).
- Procedures and assumptions adopted in developing the models (physical or probabilistic).
- Statistical uncertainty resulting from the estimation of model parameters.

Therefore, uncertainty can arise from multiple sources; distinguishing between its sources and their relative contributions facilitates decision-making to obtain meaningful results. Uncertainty can be coarsely classified either as “epistemic” or “aleatoric.” Aleatoric is derived from the Latin word *alea*, which is associated with randomness, while epistemic is derived from the Greek word *episteme*, which is related to the lack of data (Der Kiureghian and Ditlevsen 2009). Unfortunately, there is no consensus among engineers and statisticians on the correct partitioning of uncertainty into its aleatoric and epistemic components (Faber 2005; Vrouwenvelder 2003; Lindley 2000; Paté-Cornell 1996). So, the following two subsections describe how we attribute uncertainty to these two classes of uncertainty in this work.

**Epistemic Uncertainty.** We define epistemic uncertainty as the uncertainty introduced because of the lack of a priori knowledge of which the available deterministic DCA models will produce the best forecast. Our estimate of the epistemic uncertainty for each shale basin is the range between minimum and maximum deterministic forecasts derived from applying all the DCA models, as illustrated graphically in Fig. 5.

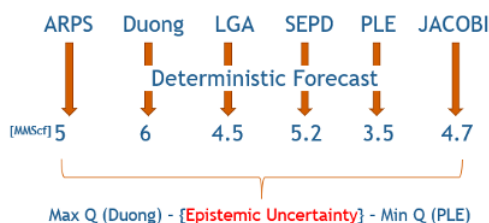


Fig. 5—Epistemic uncertainty.

**Aleatoric Uncertainty.** In this work, the aleatoric uncertainty is the uncertainty introduced because of the randomness in the production data as modeled with the combination of a particular algorithm and a given DCA model. This uncertainty is represented by the P10–P90 interval, as illustrated in Fig. 6.

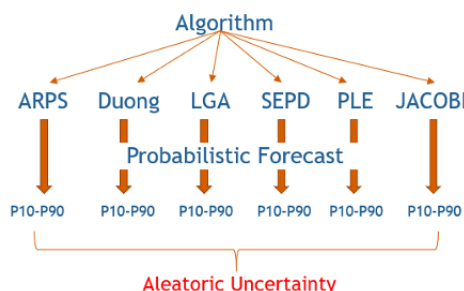


Fig. 6—Aleatoric uncertainty.

A critical insight we can provide in this work is whether a specific DCA model-stochastic algorithm pair (aleatoric uncertainty) encompasses the epistemic uncertainty described above. In situations where such pairs exist, the engineer would not have to always find the model that best matches the available data (as this objective can be a moving target). As opposed to finding the model with the best fit to the historical production data, the engineer would rather aim to find the best DCA model-stochastic algorithm pair that encompasses epistemic uncertainty.

## Well and Basin Characteristics

This section summarizes the characteristics/properties of the wells from the six shale basins studied. To give a visual indication of the location of all the wells in each basin relative to each other, we provide spatial plots of the location of the 300 wells in each shale play.

**Well Characteristics.** The completion information for the wells studied includes the fluid treatment type, treatment concentration, well location, and measured depth (MD). The range of variables considered for the well completion sensitivity analysis is shown in **Tables 3 and 4**. In **Table 3**, the treatment concentration, which is the concentration of solids in the hydraulic fracturing (or treatment) fluid in pounds of proppant per gallon of clean fluid, is treated as a categorical variable or value. This means that instead of using the real number values of the treatment concentration, we bin it into a maximum of five classes, with each class having the ranges shown in the second column of the table. The MDs in **Table 4** are also treated as categorical variables. We split the geolocation of the wells into four quadrants using the extreme data points as the quadrilateral perimeter bounds, as shown in **Fig. 7**.

Treatment Concentration	Value
Conc-1	0–0.5 ppg
Conc-2	0.5–1 ppg
Conc-3	1–1.5 ppg
Conc-4	1.5–2 ppg
Conc-5	>2 ppg

Table 3—Categorical values for the concentration ranges analyzed.

Name	MD
Depth-1	0–4,999 ft
Depth-2	5,000–9,999 ft
Depth-3	10,000–14,999 ft
Depth-4	15,000–20,000 ft
Depth-5	>20,000 ft

Table 4—Categorical values for the well MD ranges analyzed.

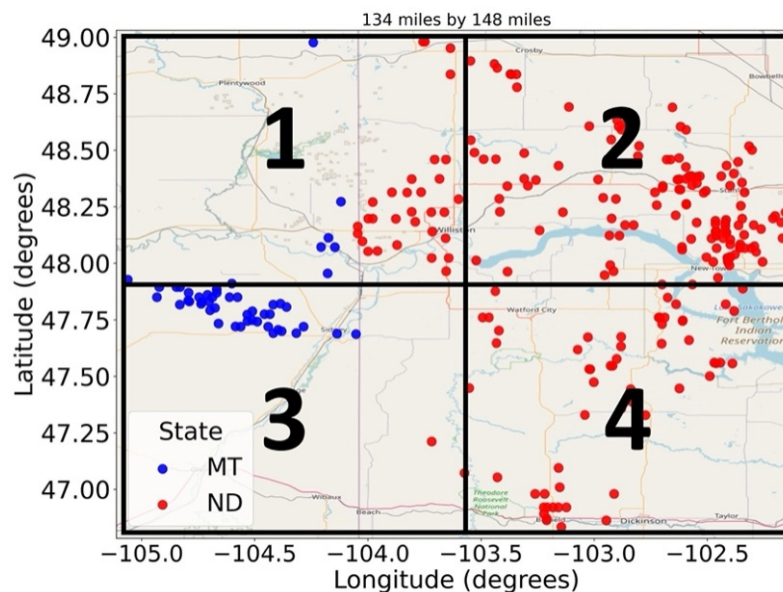
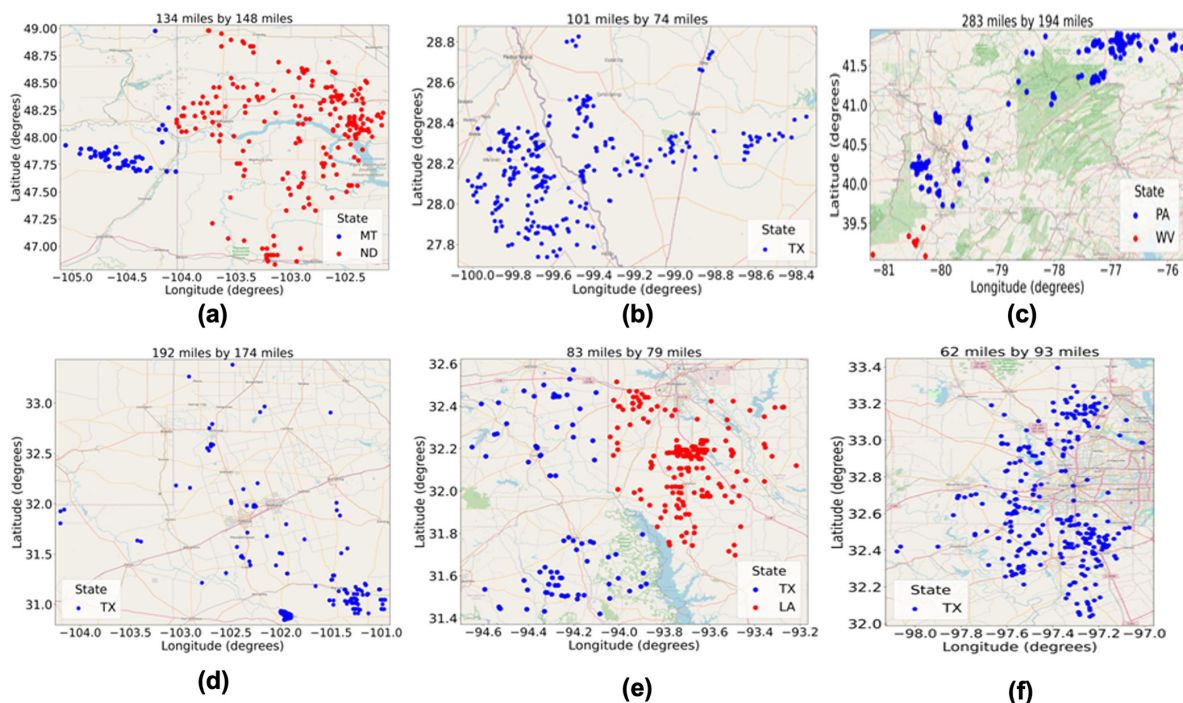


Fig. 7—Clustering of well locations.

**Basin Characteristics.** **Fig. 8** presents the bottomhole location of the 300 multistage fractured horizontal wells in the Bakken, Barnett, Eagle Ford, Haynesville, Marcellus, and Permian basins. It shows that the wells are more clustered together in some basins (like the Eagle



**Fig. 8**—This figure presents the bottomhole well locations in the Bakken, Barnett, Eagle Ford, Haynesville, Marcellus, and Permian basins, respectively (a–f). The two distances provided above each subfigure correspond to the longitudinal and latitudinal distances, respectively.

Ford) than others. Although **Table 5** only summarizes the characteristics of the wells in the Bakken Shale, Tables S-1 through S-5 in the Supplementary Materials provided with this paper summarize the characteristics of the other shale plays studied.

Characteristics	Values	Count
Well size	300	
Production type	Oil	49
	Oil and gas	251
State	North Dakota (ND), Montana (MT)	
Basin	Williston	
Mean/standard deviation oil gravity ( $^{\circ}$ API)	41.6/2.36	215
Producing reservoir	Middle Bakken (Bakken Pool), Middle Bakken/Three Forks, Three Forks, Bakken Pool, Middle Bakken (Sanish Pool), Upper Bakken, Bakken	
Treatment type	Linear gel, slickwater, crosslink, hybrid	
Mean/standard deviation proppant (lbs)	2,388,551/1,157,840	277
Mean/standard deviation treatment fluid (bbl)	41,977.09/25,065.89	271
Mean/standard deviation MD (ft)	18,842/2,531	297

Table 5—Well characteristics for the Bakken Shale.

## Discussion of Results

This section discusses the metrics we used to quantify the performance of the different probabilistic approaches used in this work. Next, we considered model and algorithmic performance as a function of hindcast length, using results from the Bakken Shale as a point of reference. We also discussed the effect of IPs and specific completion properties on probabilistic model/algorithmic performance. Last, we compared aleatoric and epistemic uncertainty.

**Evaluation Metrics.** We evaluated the performance of each probabilistic model forecast using the mean absolute prediction error (MAPE), CR, and relative error (RE). The MAPE is the mean absolute difference between the P50 prediction (or the deterministic prediction for epistemic uncertainty) and the actual data. It indicates the degree of offset of our forecast from the real data. The CR tells us what percentage of the probabilistic forecast bounds for each shale envelops the actual production, and hence, the reliability of our forecast. Since we are working with an 80% prediction interval (P90–P10), the ideal CR will be approximately 80%. Finally, the RE

metric indicates where the error leans relative to the actual production. It can either be below (underpredictive) or above (overpredictive) the actual production. **Table 6** summarizes the description and equation for the MAPE, CR, and RE metrics.

Metric	Description	Equation
MAPE/prediction error	This is the mean absolute difference between the P50 prediction and actual data.	$\frac{\sum_1^N \frac{\text{abs}(P_{50}-P_{\text{actual}})}{P_{\text{actual}}}}{N}$
CR	It is computed as a function of the indicator function, $I()$ .	$\frac{\sum_1^N I(P_{90}<P_{\text{actual}}<P_{10})}{N}$
RE	It indicates where the error leans relative to the actual production.	$\frac{\sum_1^N (P_{50}-P_{\text{actual}})}{N}$

Table 6—Metrics for evaluating algorithm and model performance.

**Sample and Iteration Size.** Fig. 9 shows the sensitivity analysis result for the various probabilistic methods using varying sample sizes. There was no notable change in the prediction error for the BS and MBS approaches, so we used a BS sample size of 500 to ensure sufficient sampling while considering the computational time. We did not run the Gibbs sampler for iterations less than 10,000 because we observed from previous work (Korde et al. 2021) that convergence for this application is usually guaranteed when the number of iterations is at least 10,000 for the Gibbs sampler. The ABC algorithm showed the lowest error with 1,000 iterations, and the error remained unchanged above 5,000 iterations. We used 10,000 iterations to ensure enough iterations comparable with the Gibbs approach. **Table 7** shows the sample size used for the various probabilistic methods.

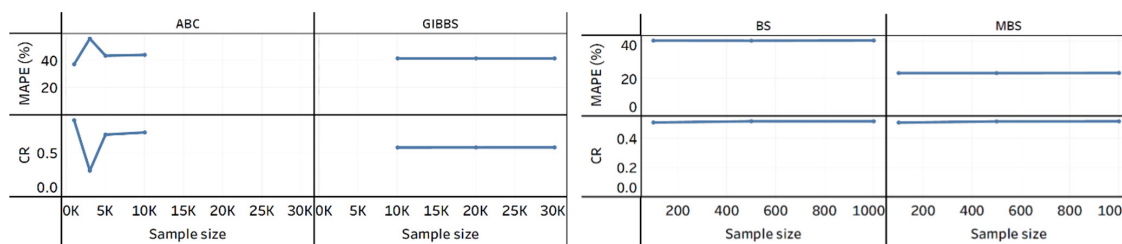


Fig. 9—Evaluation metric variation for the different probabilistic approaches.

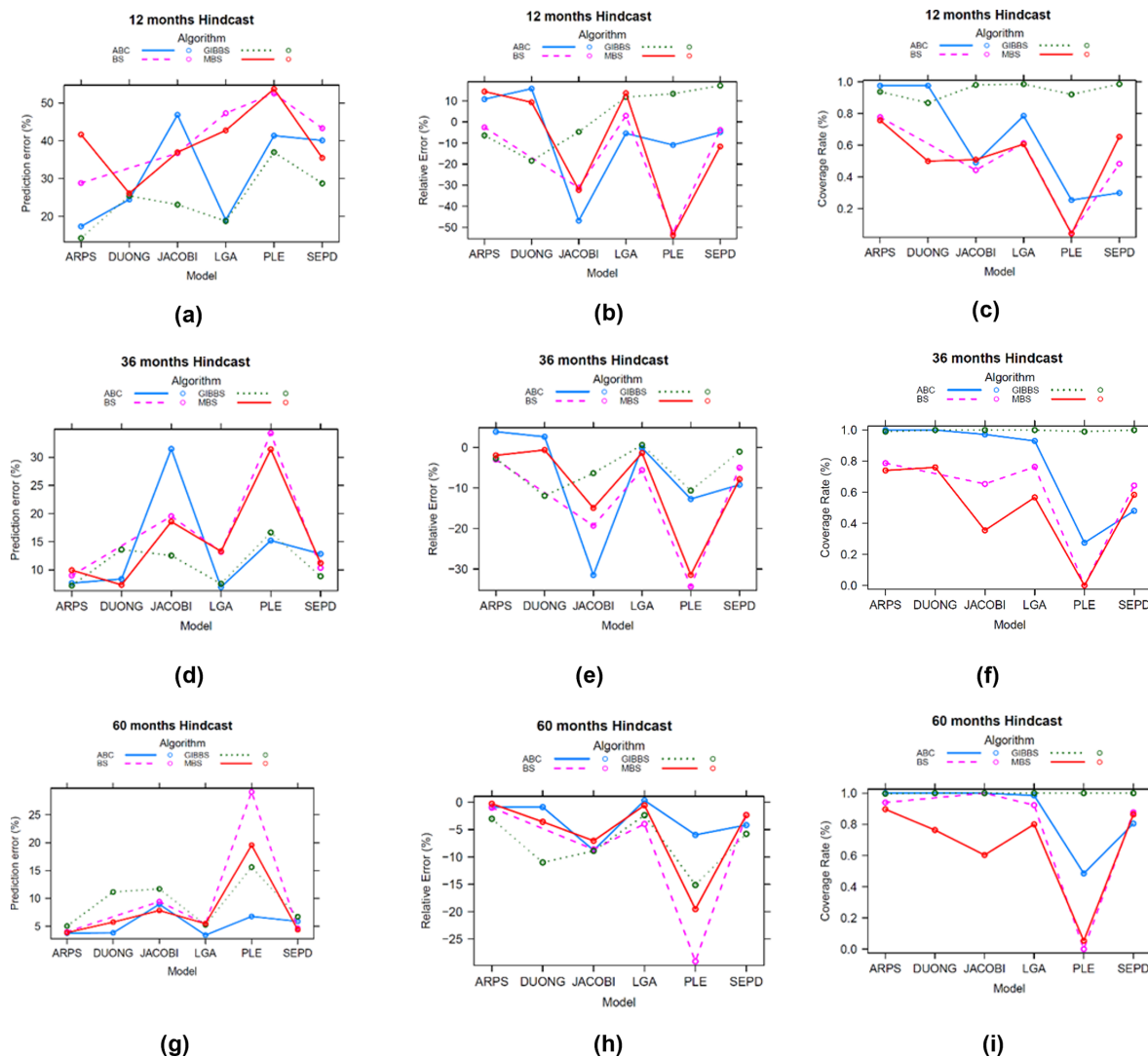
Probabilistic Algorithms	BS Sample Size for Frequentist Methods/Iteration Size for Bayesian Methods
ABC	10,000
Gibbs	10,000
BS	500
MBS	500

Table 7—Sample/iteration size used for the various probabilistic techniques.

There was no significant difference in the results from each shale basin, so we presented only the analysis results for the Bakken Shale play. Additionally, we do not include the Duong model and the BS results in these figures because they showed exceptionally large prediction errors. We will investigate this further in future work. For completeness, the analyses of the other shale basins are presented in Figs. S-1 through S-34 and Tables S-6 through S-15 of the Supplementary Materials.

**Model Performance.** Fig. 10 presents plots of the prediction error, RE, and CR for the ABC, BS, Gibbs, and MBS algorithms against the six DCA models used in this work. The four-line plots in each subfigure correspond to the ABC, BS, Gibbs, and MBS algorithms. The three rows of this figure correspond to the results obtained using only the first 12, 36, and 60 months of observed production data. These results were obtained from the Bakken Shale Basin and indicated the following:

- Specific DCA models perform better than others, especially at shorter hindcast lengths (12 months). In general, the Arps and the Duong models result in better prediction errors than the other DCA models at a hindcast of 12 months. At a hindcast of 36 months, the Arps, Duong, LGA, and SEPD models better fit the production data, as seen in the prediction errors. At 60 months, the performance disparity between the most DCA models becomes less significant.
- The empirical DCA models were the best performing models. They vastly outperformed the analytical Jacobi model except for the PLE model.
- The prediction error reduces with increasing hindcast length for each DCA model while the RE trends toward neutrality (0%).
- The CR gets better as more historical production data become available, implying that the DCA model predictions become better calibrated with increasing hindcast lengths.
- The PLE model performed the worst across all hindcast lengths for each evaluation metric.
- Specific DCA models, such as the PLE and Jacobi, are significantly pessimistic. In contrast, others are either pessimistic or optimistic, depending on the combination of the probabilistic algorithm and the DCA model.



**Fig. 10—Effect plot of algorithm performance with different DCA models at selected hindcast sizes for the Bakken Shale.**

Although these observations are illustrated using the results from the analysis of the Bakken Shale, comparable results were observed for the other six shale basins, as shown in Figs. S-1 through S-34 and Tables S-6 through S-15 of the Supplementary Materials provided with this paper.

**Algorithm Performance.** Fig. 11 presents the prediction error, RE, and CR for the six DCA models plotted against the ABC, BS, Gibbs, and MBS algorithms. As in Fig. 10, the three rows of this figure correspond to the results obtained using the first 12, 36, and 60 months of observed production data only. Although the same data are used to generate Figs. 10 and 11, the former plots the probabilistic algorithms as line plots against the DCA models on the x-axis, while the latter plots the DCA models as line plots against the probabilistic algorithms on the x-axis. The results presented in Fig. 11 indicate that:

- The Bayesian algorithms (ABC or Gibbs or both) perform best in terms of the prediction error at short hindcast lengths (12 months hindcast).
- As the hindcast length increases, the difference between the algorithm performance reduces. At longer hindcast lengths, all the algorithms show similar prediction errors, except algorithms associated with the Duong model.
- The prediction error reduces with increasing hindcast length for each algorithm, while RE trends toward neutrality (0%).
- The CR generally increases as more historical production data are available.

Table 8 presents the model-algorithm combination with the lowest prediction error. It shows that the Bayesian algorithms outperform the frequentist algorithm in terms of prediction error. In contrast, Table 9 shows that the frequentist algorithms outperform the Bayesian algorithms in terms of the CR. We used a prediction interval of 80% for our probabilistic forecast; therefore, a CR of approximately 80% is desirable.

**Effect of IPs.** Fig. 12 presents the MAPE and CR for the ABC and Gibbs algorithms with and without IP probabilistic distributions. The suffixes IP and NIP after the ABC and Gibbs algorithms (in the legend) represent the *informative prior* and *noninformative prior* probabilistic distributions. The figure shows that using IPs in the ABC and Gibbs algorithms results in a significant improvement in the performance of these algorithms compared with NIP (or uniform) distributions. The top plot in Fig. 12 shows a significant (~50%) reduction in the prediction error when IPs are used. This result shows how sensitive the Bayesian methodology is to the prior distributional

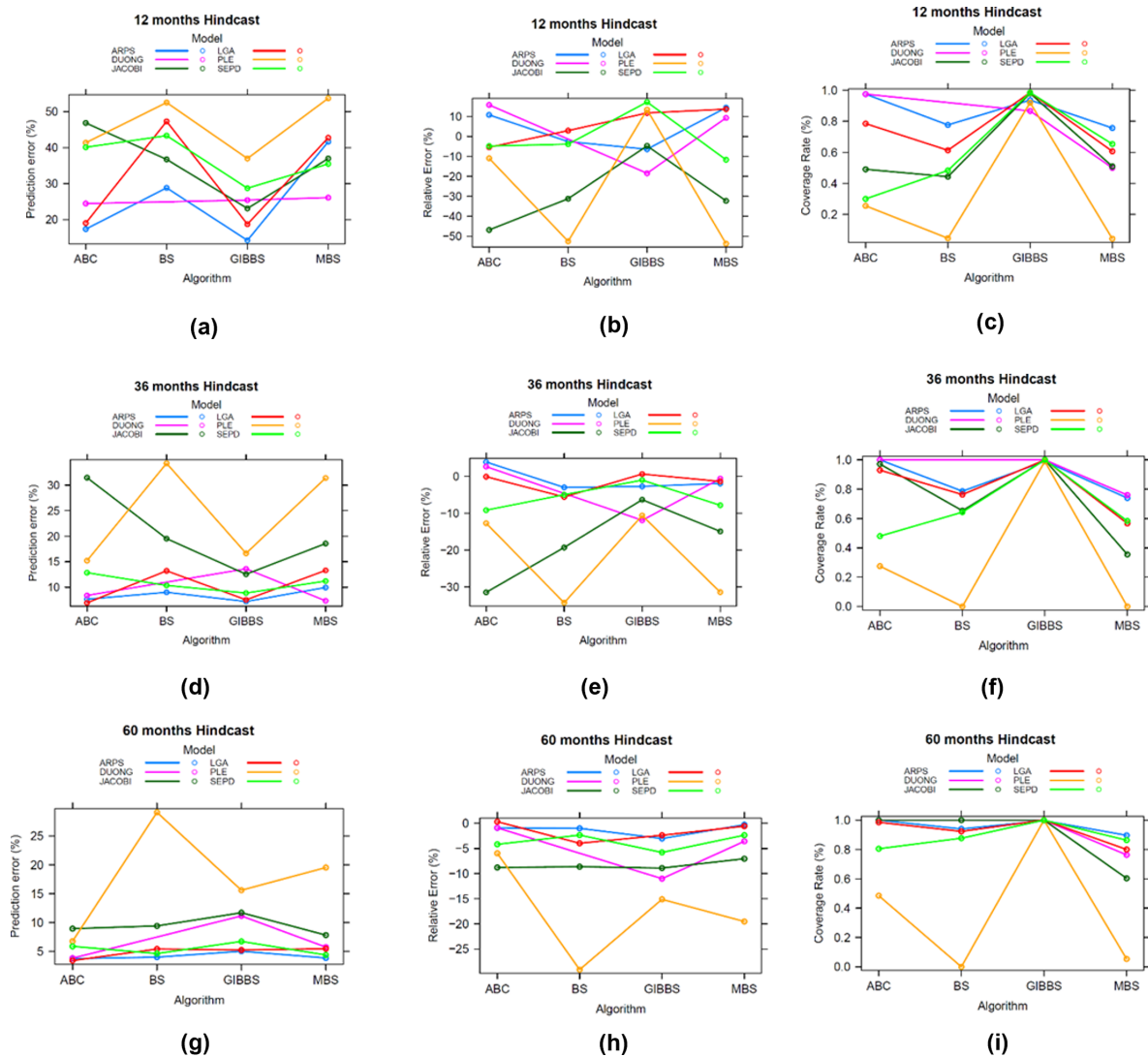


**Fig. 11—Effect plot of DCA performance with different algorithms at selected hindcast size for the Bakken Shale.**

Hindcast (months)	Pair	Prediction Error (%)	CR (%)
12	Gibbs-Arps	14.22	94
36	ABC-LGA/Arps-Gibbs	6.93/~7	93
60	ABC-LGA	3.40	99

**Table 8—Best performing model combination based on the prediction error in the Bakken Basin.**

Hindcast (months)	Pair	CR (%)	Prediction Error (%)
12	ABC-LGA	79	19.02
36	BS-Arps	79	9
60	MBS-LGA	80	5.46

**Table 9—Best performing model combination based on the CR in the Bakken basin.**

assumptions, which may be one of the reasons the Bayesian algorithms outperform their frequentist counterparts in this work. The bottom plot in this figure shows an improvement in the CR when IPs are used instead of NIPs.

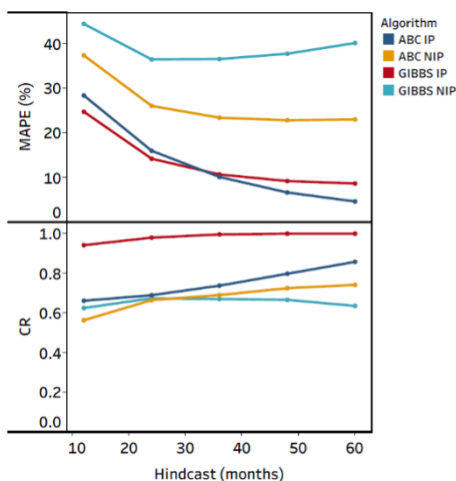


**Fig. 12**—Performance of Bayesian algorithms (ABC and Gibbs) with IPs and NIPs for the Bakken Shale. This plot is an aggregate of all DCA models.

**Fig. 13** presents the MAPE and CR for each DCA model and stochastic algorithm combination. The results confirm the reduction in MAPE for virtually all pairs of DCA models and stochastic algorithms, but the effect of IPs is more significant in specific DCA models than others. The prediction error for the Jacobi-Gibbs pair with NIP was so high that we excluded it from the plot. Additionally, we observe that the CR is generally higher under IPs for all combinations of DCA models and stochastic algorithms, except the Jacobi-ABC combination. Although **Figs. 12 and 13** present the results for the Bakken Shale, **Figs. S-6, S-7, S-13, S-14, S-20, S-21, S-27, and S-28** in the Supplementary Materials show the corresponding results for other shale basins. These results indicate the importance of computing and using IP distributions in probabilistic DCA for unconventional reservoirs.

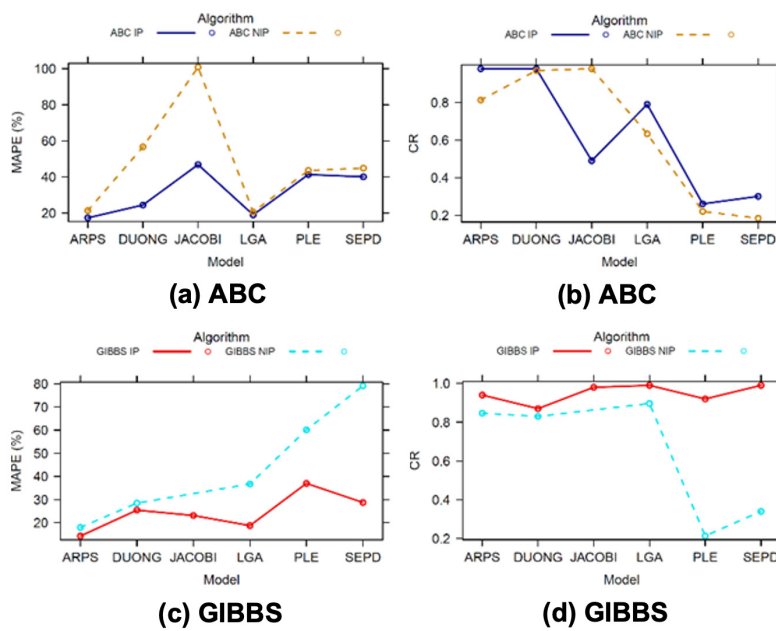


**Fig. 13**—Effect of IPs on DCA models with Bayesian algorithms (ABC and Gibbs) for the Bakken Shale at 12 months hindcast.

**Performance Correlation with Well Completion Properties.** **Fig. 14** presents the performance of the four probabilistic algorithms when different fluid treatment types (**Fig. 14a**), treatment concentrations (**Fig. 14b**), well MDs (**Fig. 14c**), and well locations (**Fig. 14d**) are considered. The plots presented in **Fig. 14a** show that the MAPE and CR are consistent across all fluid treatment types regardless of the algorithm used and the imbalance in the data, as indicated by the well count for each fluid treatment type. A similar consistency is observed in the performance of the probabilistic algorithms when different treatment concentrations, well depths, and well locations are considered in **Figs. 14b through 14d**, respectively. We also observe from **Fig. 14** that the CR centers around 0.8 for the ABC algorithm, which is the 80% prediction interval adopted in our probability bounds. The Gibbs algorithm shows a nearly 100% CR, whereas those of the BS and MBS are lower than the 80% prediction interval.

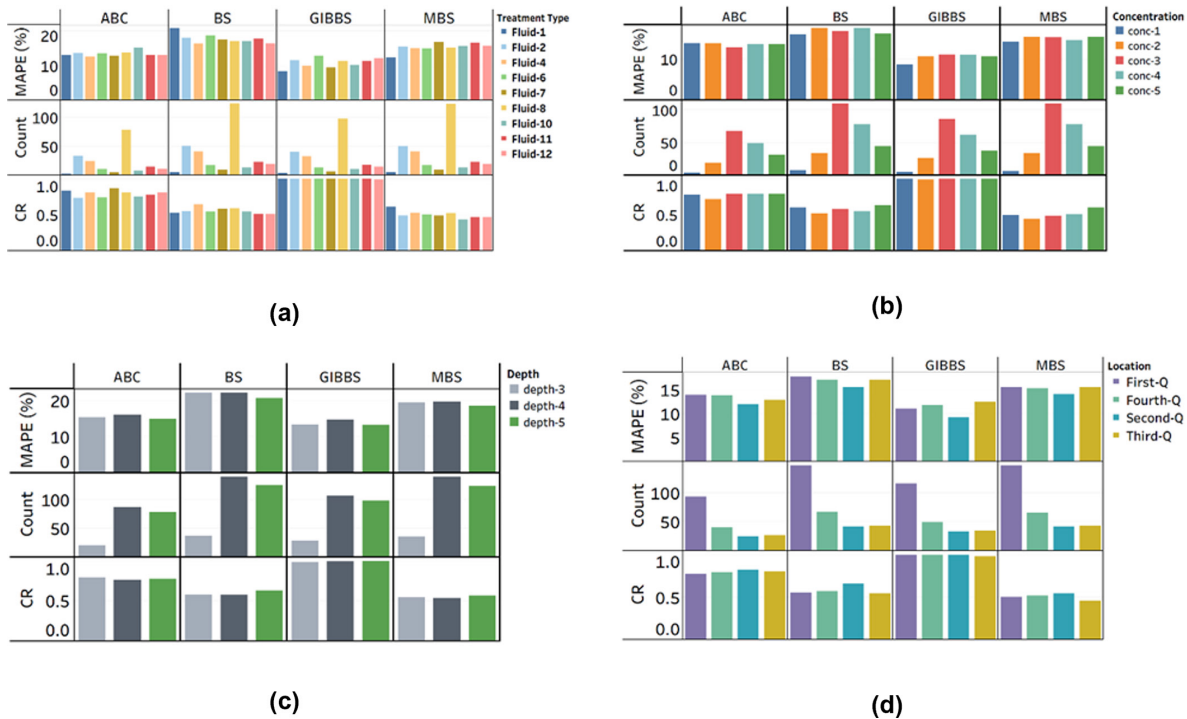


**Fig. 14—Algorithm performance across various operational and reservoir location properties for the Bakken Shale. This plot aggregates all DCA model performances captured at a 36-month hindcast.**

### Epistemic DCA Model Uncertainty vs. Aleatoric Algorithm Uncertainty

**Fig. 15** presents box plots showing the range of aleatoric and epistemic uncertainties associated with the four probabilistic algorithms. The plots shown in **Figs. 15a through 15d** were obtained using a 36-month hindcast on the production data from 200 Bakken Shale wells. The first six boxes in each of the four plots depict the variability among the forecasted cumulative production from the 200 wells, thus conveying the aleatoric uncertainty associated with each of the six DCA models displayed on the *x*-axis. The last box represents epistemic uncertainty and is shown as “EPIS” on the *x*-axis. The forecast production volumes indicated on the *y*-axis in this figure were presented in barrels, while the blue, orange, and red dots in each box plot represent the P10, P50, and P90 cumulative production forecasts on a per well basis. Although the aleatoric uncertainties associated with the DCA models vary from plots (a) through (d) in **Fig. 15**, the epistemic uncertainty shown is identical in all four plots. The epistemic uncertainty is independent of probabilistic algorithms and added here solely for easy comparison. This is because the epistemic uncertainty is computed from the aggregation of all six DCA models. For each DCA model, we calculated the average cumulative production from the 200-well data set. This resulted in a single average cumulative production statistic per DCA model per basin. The epistemic uncertainty is calculated from concatenating the cumulative production statistic from all six DCA models and presenting them in a box plot format.

Given the background in the previous paragraph, we propose the following thought experiment. Suppose an engineer wants to predict the cumulative production from a given well in the Bakken Shale. The engineer wishes to know if there exists a DCA-stochastic algorithm combination whose aleatoric uncertainty encompasses the epistemic uncertainty associated with cumulative production forecasts for this well. If such a combination exists, the engineer does not need to apply six different DCA algorithms to the production data to obtain a priori knowledge of the forecast uncertainty. **Fig. 15** provides results that can be analyzed to determine if this DCA-stochastic algorithm combination exists.

We start this analysis of **Fig. 15** by noting that the last box plot in each quadrant represents epistemic uncertainty. Therefore, from **Figs. 15a through 15d**, we need to find which one of the DCA-stochastic algorithm combinations encompasses epistemic uncertainty. This is achieved by simply comparing the range of the DCA-stochastic algorithm box plot with that of the epistemic uncertainty and selecting the one(s) where the range of the epistemic uncertainty lies within that of the DCA-stochastic algorithm combination. If multiple DCA-stochastic algorithm box plots encompass the epistemic uncertainty box plot, we choose the one that is closest to the range of the epistemic uncertainty (i.e., the one with the tightest bounds). In **Fig. 15a**, none of the DCA-stochastic algorithm combinations (aleatoric uncertainty) encompasses epistemic uncertainty, while in **Fig. 15b**, most of the DCA-stochastic algorithm combinations encompass epistemic uncertainty. Based on the criteria for choosing the combination with the tightest bounds, in this case, the Arps-Gibbs combination is considered the best choice in **Fig. 15b**. Using this reasoning for **Figs. 15a through 15d** suggests that the DCA-stochastic algorithm combinations that most tightly encompass the epistemic uncertainty in the Bakken are the Arps-Gibbs, Jacobi-BS, and the Arps-ABC combinations. Comparing the uncertainty ranges of these three DCA-stochastic algorithm combinations, the Jacobi-BS fits the epistemic uncertainty most tightly. Therefore, for an engineer working on forecasting the production performance of Bakken Shale oil wells, our recommended DCA-stochastic algorithm combination that encompasses epistemic uncertainty would be the Jacobi-BS.

The above reasoning is repeated for the other shale basins investigated, and the results are summarized in **Table 10** (also see Figs. S-3, S-12, S-19, S-26, and S-33 in the Supplementary Material provided). Despite the preceding, the answer to the question of whether an engineer should focus on the determination of the “best” model out of the plethora of available DCA models (reflecting the epistemic uncertainty) or should spend more time and effort on quantifying the aleatoric uncertainty will still depend on the philosophical bent and inclination of the engineer. Engineers who favor the “best model” approach do not need to change their current workflow. However, for engineers whose philosophical bent subscribes to Voltaire’s perfection-being-the-enemy-of-good aphorism and who wish to quantify the aleatoric uncertainty while still respecting the epistemic uncertainty range, we believe **Table 10** offers valuable guidance.

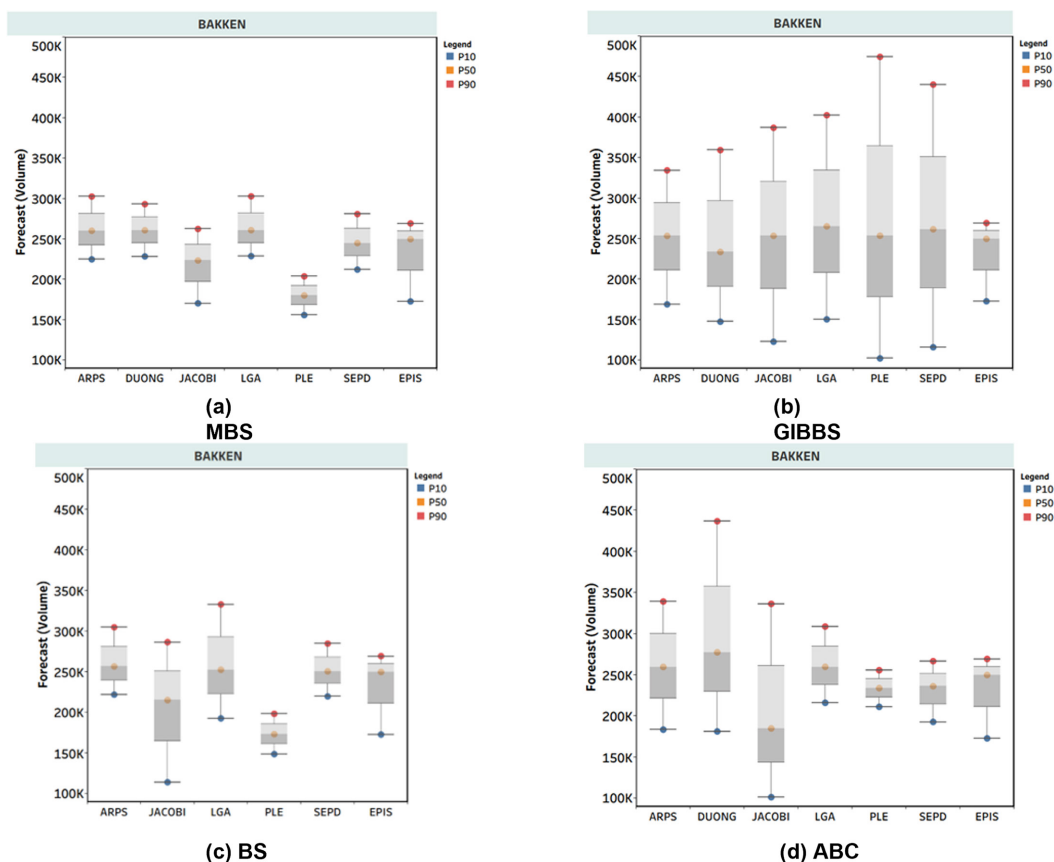


**Fig. 15—A comparison of aleatoric and epistemic uncertainty in the Bakken shale play. The aleatoric quantification method in (a) is MBS, in (b) is Gibbs, in (c) is BS, and in (d) is ABC. Forecast volumes are in barrels.**

Shale	Model Combination
Bakken oil	Arps-Gibbs/Jacobi-BS/Arps-ABC
Barnett gas	Jacobi-BS
Eagle Ford oil	SEPD-Gibbs
Haynesville gas	SEPD-ABC/Jacobi-MBS
Marcellus gas	Jacobi-BS/Jacobi-ABC/LGA-Gibbs
Permian oil	SEPD-ABC

**Table 10—Aleatoric uncertainty model combinations that encompass epistemic uncertainty on a shale-by-shale basis for a 36-month hindcast.**

## Conclusions

Based on the results presented in this work, we conclude the following:

- The Arps and Duong models generally yield lower prediction errors than the other DCA models at a hindcast of 12 months for most of the stochastic algorithms studied. At a hindcast of 36 months, the Arps, Duong, LGA, and SEPD models better fit the production data as indicated by the prediction errors. At 60 months, the performance disparity between most DCA models becomes less significant.
- The empirical DCA models were the best performing models. They vastly outperformed the analytical Jacobi model except for the PLE model. We also observed that the PLE and Jacobi models are consistently and significantly pessimistic. In contrast, the others are either pessimistic or optimistic, depending on the probabilistic algorithm and the DCA model.
- As expected, the prediction error reduces with increasing hindcast length for each DCA model, the RE trends toward neutrality (0%), and the CR improves as more historical production data become available. This implies that the DCA model predictions become more reliable with increasing hindcast lengths, as expected.
- The Bayesian algorithms (ABC or GIBBS or both) outperform the others in terms of the prediction error at short hindcast lengths (12-month hindcast). As the hindcast length increases, the difference in predictive performance between the algorithms reduces. At longer hindcast lengths, all the algorithms show a similar level of prediction errors, with the significant exception of the algorithms associated with the PLE model.
- We found that the use of IPs significantly influences the performance of the Bayesian algorithms when compared with NIPs (uniform distribution). The amount of production history available is the common deciding factor in the model and algorithm predictive

performance. When there are sufficient production data (defined as between three-eighths and five-eighths of the complete production history), less concern needs to be paid to the choice of model or algorithm.

- Varying completion properties did not influence the predictive performance of the probabilistic algorithms investigated in this work.
- We found that there exists a DCA-stochastic algorithm combination (aleatoric uncertainty) that encompasses the estimated epistemic uncertainty for most of the shale basins investigated. Interested engineers can use this suggested combination to represent the epistemic uncertainty associated with the corresponding shale basin forecasts.

## Nomenclature

All symbols used in the paper are defined clearly with dimensions and units (as applicable) at first mention in the text.

## References

- Arps, J. J. 1945. Analysis of Decline Curves. *Trans.* **160** (1): 228–247. SPE-945228-G. <https://doi.org/10.2118/945228-G>.
- Begg, S. H., Welsh, M. B., and Bratvold, R. B. 2014. Uncertainty vs. Variability: What's the Difference and Why Is It Important? Paper presented at the SPE Hydrocarbon Economics and Evaluation Symposium, Houston, Texas, USA, 19–20 May. SPE-169850-MS. <https://doi.org/10.2118/169850-MS>.
- Cheng, Y., Wang, Y., McVay, D. A. et al. 2010. Practical Application of a Probabilistic Approach to Estimate Reserves Using Production Decline Data. *SPE Econ & Mgmt* **2** (1): 19–31. SPE-95974-PA. <https://doi.org/10.2118/95974-PA>.
- Choi, J., Kim, D., and Byun, J. 2020. Uncertainty Estimation in Impedance Inversion Using Bayesian Deep Learning. Paper presented at the SEG Technical Program Expanded Abstracts 2020, Virtual, 13 October. <https://doi.org/10.1190/segam2020-3428098.1>.
- Clark, A. J., Lake, L. W., and Patzek, T. W. 2011. Production Forecasting with Logistic Growth Models. Paper presented at the SPE Annual Technical Conference and Exhibition, Denver, Colorado, USA, 30 October–2 November. SPE-144790-MS. <https://doi.org/10.2118/144790-MS>.
- Csilléry, K., Blum, M. G. B., Gaggiotti, O. E. et al. 2010. Approximate Bayesian Computation (ABC) in Practice. *Trends Ecol Evol* **25**: 410–418. <https://doi.org/10.1016/j.tree.2010.04.001>.
- Der Kiureghian, A. and Ditlevsen, O. 2009. Aleatory or Epistemic? Does It Matter? *Struct Saf* **31** (2): 105–112. <https://doi.org/10.1016/j.strusafe.2008.06.020>.
- Duong, A. N. 2011. Rate-Decline Analysis for Fracture-Dominated Shale Reservoirs. *SPE Res Eval & Eng* **14** (3): 377–387. SPE-137748-PA. <https://doi.org/10.2118/137748-PA>.
- Faber, M. H. 2005. On the Treatment of Uncertainties and Probabilities in Engineering Decision Analysis. *J Offshore Mech Arct Eng* **127** (3): 243–248. <https://doi.org/10.1115/1.1951776>.
- Farooq, U., Hazlett, R. D., and Babu, D. K. 2020. Rate Transient Analysis of Arbitrarily-Oriented, Hydraulically-Fractured Media. *J Comput Appl Math* **379**: 112966. <https://doi.org/10.1016/j.cam.2020.112966>.
- Gong, X., Gonzalez, R., McVay, D. A. et al. 2014. Bayesian Probabilistic Decline-Curve Analysis Reliably Quantifies Uncertainty in Shale-Well-Production Forecasts. *SPE J.* **19** (6): 1047–1057. SPE-147588-PA. <https://doi.org/10.2118/147588-PA>.
- Gonzalez, R. A., Gong, X., and McVay, D. A. 2012. Probabilistic Decline Curve Analysis Reliably Quantifies Uncertainty in Shale Gas Reserves Regardless of Stage of Depletion. Paper presented at the SPE Eastern Regional Meeting, Lexington, Kentucky, USA, 3–5 October. SPE-161300-MS. <https://doi.org/10.2118/161300-MS>.
- Hazlett, R. D. and Babu, D. K. 2014. Discrete Wellbore and Fracture Productivity Modeling for Unconventional Wells and Unconventional Reservoirs. *SPE J.* **19** (1): 19–33. SPE-159379-PA. <https://doi.org/10.2118/159379-PA>.
- Hazlett, R. D. and Babu, D. K. 2018. Transient-Inflow-Performance Modeling From Analytic Line-Source Solutions for Arbitrary-Trajectory Wells. *SPE J.* **23** (3): 906–918. SPE-189463-PA. <https://doi.org/10.2118/189463-PA>.
- Hazlett, R. D., Farooq, U., and Babu, D. K. 2021. A Complement to Decline Curve Analysis. *SPE J.* **26** (4): 2468–2478. SPE-205390-PA. <https://doi.org/10.2118/205390-PA>.
- Holanda, R. W., Gildin, E., and Valko, P. P. 2018. Mapping the Barnett Shale Gas With Probabilistic Physics-Based Decline Curve Models and the Development of a Localized Prior Distribution. Paper presented at the SPE/AAPG/SEG Unconventional Resources Technology Conference, Houston, Texas, USA, 23–25 July. URTEC-2902792-MS. <https://doi.org/10.15530/urtec-2018-2902792>.
- Hubbard, D. W. 2014. *How to Measure Anything*. Hoboken, New Jersey, USA: Wiley. <https://doi.org/10.1002/9781118983836>.
- Ilk, D., Rushing, J. A., Perego, A. D. et al. 2008. Exponential vs. Hyperbolic Decline in Tight Gas Sands — Understanding the Origin and Implications for Reserve Estimates Using Arps' Decline Curves. Paper presented at the SPE Annual Technical Conference and Exhibition, Denver, Colorado, USA, 21–24 September. SPE-116731-MS. <https://doi.org/10.2118/116731-MS>.
- Jochen, V. A. and Spivey, J. P. 1996. Probabilistic Reserves Estimation Using Decline Curve Analysis with the Bootstrap Method. Paper presented at the SPE Annual Technical Conference and Exhibition, Denver, Colorado, USA, 6–9 October. SPE-36633-MS. <https://doi.org/10.2118/36633-MS>.
- Khanal, A., Khoshghadam, M., Makinde, I. et al. 2015. Modeling Production Decline in Liquid Rich Shale (LRS) Gas Condensate Reservoirs. Paper presented at the SPE/CSUR Unconventional Resources Conference, Calgary, Alberta, Canada, 20–22 October. SPE-175913-MS. <https://doi.org/10.2118/175913-MS>.
- Korde, A., Goddard, S. D., and Awoleke, O. O. 2021. Probabilistic Decline Curve Analysis in the Permian Basin Using Bayesian and Approximate Bayesian Inference. *SPE Res Eval & Eng* **24** (3): 536–551. SPE-204477-PA. <https://doi.org/10.2118/204477-PA>.
- Lee, J. and Sidle, R. 2010. Gas-Reserves Estimation in Resource Plays. *SPE Econ & Mgmt* **2** (2): 86–91. SPE-130102-MS. <https://doi.org/10.2118/130102-PA>.
- Lindley, D. V. 2000. The Philosophy of Statistics. *J Royal Statistical Soc D* **49** (3): 293–337. <https://doi.org/10.1111/1467-9884.00238>.
- Makinde, I. and Lee, W. J. 2016. Production Forecasting in Shale Volatile Oil Reservoirs Using Reservoir Simulation, Empirical and Analytical Methods. Paper presented at the SPE/AAPG/SEG Unconventional Resources Technology Conference, San Antonio, Texas, USA, 1–3 August. URTEC-2429922-MS. <https://doi.org/10.15530/urtec-2016-2429922>.
- Okoli, C. 2020. *Uncertainty Quantification in Unconventional Reservoirs Using Conventional Bootstrap and Modified Bootstrap Methodology*. MSc Thesis, University of Alaska, Fairbanks, Alaska, USA.
- Okouma, V., Symmons, D., Hosseinpour-Zonoozi, N. et al. 2012. Practical Considerations for Decline Curve Analysis in Unconventional Reservoirs — Application of Recently Developed Time-Rate Relations. Paper presented at the SPE Hydrocarbon Economics and Evaluation Symposium, Calgary, Alberta, Canada, 24–25 September. SPE-162910-MS. <https://doi.org/10.2118/162910-MS>.
- Paryani, M., Awoleke, O. O., Ahmadi, M. et al. 2017. Approximate Bayesian Computation for Probabilistic Decline-Curve Analysis in Unconventional Reservoirs. *SPE Res Eval & Eng* **20** (2): 478–485. SPE-183650-PA. <https://doi.org/10.2118/183650-PA>.
- Paté-Cornell, M. E. 1996. Uncertainties in Risk Analysis: Six Levels of Treatment. *Reliab Eng Syst Saf* **54** (2–3): 95–111. [https://doi.org/10.1016/S0951-8320\(96\)00067-1](https://doi.org/10.1016/S0951-8320(96)00067-1).

- R Core Team. 2020. *R: A Language and Environment for Statistical Computing*. Vienna, Austria: R Foundation for Statistical Computing. <https://www.R-project.org/>.
- Valkó, P. P. and Lee, W. J. 2010. A Better Way to Forecast Production from Unconventional Gas Wells. Paper presented at the SPE Annual Technical Conference and Exhibition, Florence, Italy, 19–22 September. SPE-134231-MS. <https://doi.org/10.2118/134231-MS>.
- Vrouwenvelder, A. C. W. M. 2003. Uncertainty Analysis for Flood Defense Systems in The Netherlands. Paper presented at the Safety and Reliability. Proceedings of ESREL, European Safety and Reliability Conference 2003, Maastricht, The Netherlands, 15–18 June.